

## CFD SIMULATION AND STRUCTURE OPTIMIZATION OF THE HOT-AIR DRYING OVEN OF A GRAVURE PRINTING MACHINE

Linlin Liu\*, Chuliang Wan and Kaikai Li

Faculty of Printing, Packaging Engineering and Digital Media Technology, Xi'an University of Technology,  
Xi'an, 710048, Shanxi, China

Email: Liulinlin1978@gmail.com

### ABSTRACT

Gravure printing machines are widely used in modern printing fields due to their particular advantages. This paper establishes a multi-beam air impinging drying model for a convection drying device, and builds a CFD analysis model. Through analyses of flow traces and pressure nephograms of a drying oven, the hot-air flow state and pressure distribution characteristics are presented, corresponding to a complex structure. Based on dynamic simulation analysis, an air duct with a connecting bottom structure is provided, which effectively improves non-uniform air blowing. The air suction port in the bottom is also designed to solve the problem of organic solvent retention. To improve non-uniform circulation and increase utilization efficiency, following comparative simulation analysis, this paper puts forward a new tuyere structure with a horizontal clapboard. The optimum dimensions for this new structure are obtained. This paper also obtains the optimum interval of tuyeres and the optimum distance to surfaces of substrate, which increases drying efficiency and decreases solvent residual efficiency. This paper analyzes the performance characteristics of a drying oven and mastered drying technical parameters, hence providing evidence and support for drying system optimization and innovative design.

**Keywords:** CFD model, Fluid analysis, Gravure press, Hot air drying, Structure optimization.

### 1. INTRODUCTION

In recent years, gravure printing has been widely used in the fields of plastic packaging, paper packaging, decoration, securities printing and publishing. Its wide use is due to its thick ink layer, abundant hierarchies, stable printing quality, fast printing, wide substrates and tendency to develop rapidly [1].

Gravure ink is comprised of pigment, resin, solvent and other components. The volatilization of solvent in the ink demands a great quantity of heat consumption [2]. At present, the drying of high velocity gravure press printing mostly adopts the hot-air convection mode.

To accelerate the drying of ink and to increase printing speed, every type of gravure printing machine is provided with a drying device. The drying device is an important component of a gravure printing machine. It finishes the enforced drying of printed products within a very short time [2]. The drying efficiency of a drying device has become a key factor in restricting printing speed and quality, and is also key in affecting the performance of the whole machine [3].

The drying technique is an interdisciplinary technique with experimental properties. The structure of the drying device, the ink performance, the hot air temperature and the printing speed will all affect drying efficiency in gravure printing [4]. Within this list of factors, the hot-air dynamic characteristics and structural parameters of tuyeres in the drying device also directly affect drying efficiency [1].

### 2. MODELING A HOT-AIR DRYING DEVICE

#### 2.1 Convection drying device

Existing drying systems have three drying patterns: heat radiation drying; heat conduction drying; and heat convection drying. At present, the most widely used drying pattern in gravure printing is the latter; involving hot-air convection. The structure of the drying system of a gravure press is shown in Figure 1. The air is heated by the pipe heater; the fan then blows hot air into the drying oven, and the heated air is jetted out through a long, narrow tuyere as a result of a pressure difference. This causes the air to impact the substrate at a high speed and at a certain distance from the row of vertical (or inclined) tuyeres, which makes the solvent dry and volatilize rapidly. Finally, air is discharged from the exhaust airway. Some of the hot air then enters a second recycling circuit for second utilization [5] [6].

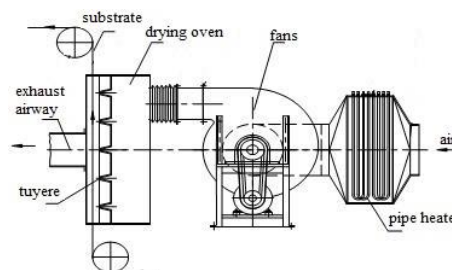


**Figure 1.** Hot-air convection drying system

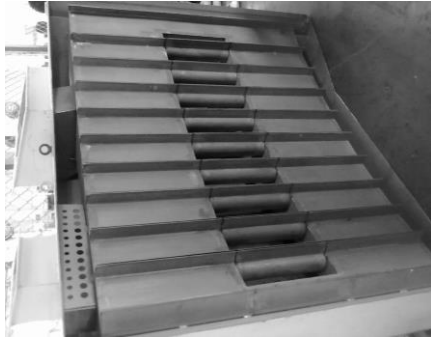


**Figure 2.** Drying oven in an FR300 gravure press

Figure 2 shows the drying oven in an FR300 gravure press. As shown, there are rows of tuyeres, which follow the multi-beam air impinging jet drying model. Jets between tuyeres here interfere with each other.

As shown in Figure 3, the air scatters on the plane and forms a wall jet area, with hot air stagnation in the middle. In a very small transitional area (the length is related to the Reynolds coefficient), close to the tuyere, high-velocity jet flow causes a shear layer. The instability of this layer grows rapidly and forms a vortex within a surrounding flow. It is closely related to hot air loss and the velocity of solvent steaming and flowing, which further affects the drying velocity [7][8].

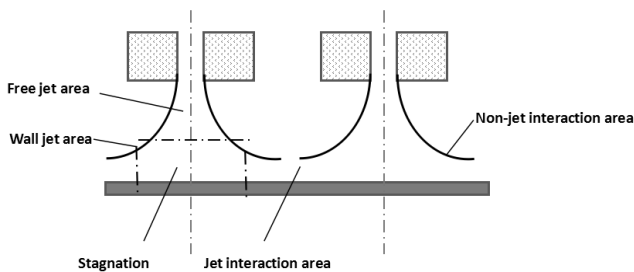


**Figure 3.** The multi-beam air impinging jet drying model

## 2.2. CFD modeling on a drying device

Under the basic control equations for fluid flow (the equations for mass, momentum and energy conservation), flow states of the fluid can be analyzed through numerical simulation. The basic equations for general hot-air flow control in the drying device can then be solved numerically [9].

In this paper, in order to approximately simulate the hot-air flow state and to optimize design of the structure, CFD was adopted to implement numerical analyses of temperature, velocity and the uniformity of fluids in the drying oven [10].

Due to the complexity of the hot-air fluid domain inside the drying device, Boolean operations should be carried out on the whole drying device to distinguish all areas of hot air flow [11]. Therefore, it should be assumed that the drying device is closed. The fluid domain of hot air is only limited inside the drying device and no loss of air speed and air pressure is considered. Errors of fabrication and assembly should be neglected and deformation problems caused by fabrication imprecision and installation should be neglected. The gridding model is then carried out, as shown in Figure 4.

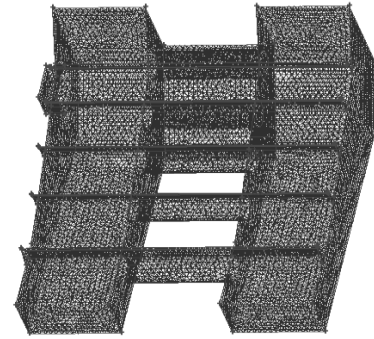


**Figure 4.** The gridding model of a hot-air drying oven

The hot air in the oven belongs to a constant viscous fluid, and meets the momentum conservation equation, the mass conservation equation and the energy conservation equation, that together control conservation.

The evidence for judging the flow pattern of the fluid, i.e., the laminar flow, or turbulence, depends on the Reynolds number and whether the fluid has surpassed the critical Reynolds number [12]. The definition of the Reynolds number is as follows in Equation (1):

$$Re = \rho \frac{VL}{\nu} \quad (1)$$

Here:  $V$  is the average speed in sections,  $L$  is the characteristic length and  $\nu$  is the kinematical viscosity of the fluid.

The Reynolds number of the hot air inlet of an FR300 drying oven model is 332,530, which is greater than the critical Reynolds number of 2,330. Therefore, this represents turbulent flow and the RNG k- $\epsilon$  model should be used for simulation calculations [12] [14].

To simplify the question, the following assumptions are made:

- (1) The fluid domain within the hot-air flow area is constant;
- (2) The flow of hot air inside the drying device is a steady turbulent flow;
- (3) The flow process of hot air in the whole fluid domain is a steady flow;
- (4) The flow rate of air at the inlet of the tuyeres is uniform and is an average value of the total flow quantity.

The discrete mode, the implicit solving equation and unsteady solution parameters are adopted [15].

## 3. HOT-AIR FLOW STATE IN A DRYING OVEN

### 3.1 Hot-air flow traces analysis in a drying oven

A chamber trace of the drying oven has been extracted after Fluent analysis. As shown in Figure 5, the flowing trace of a single mass point within a continuous process is a method of Lagrange to describe flowing. The flow state of hot air in a drying oven can be mastered intuitively through analysis of the overall and local flow trace of the drying oven.

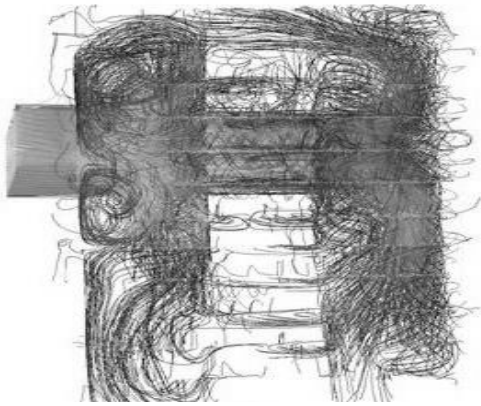


**Figure 5.** Traces map of a drying oven

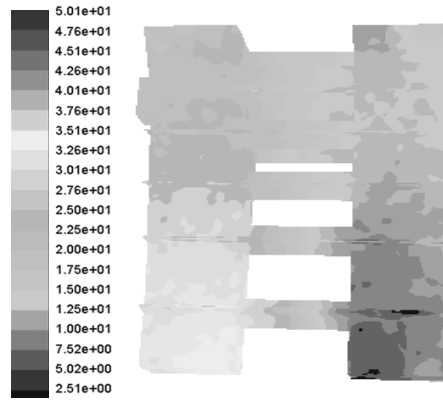


**Figure 6.** Pressure vector nephogram of a drying oven

First, hot air flows into a drying oven and the section suddenly becomes bigger. Due to the interaction between hot air and the oven, the asymmetric pressure distribution between the front and the back causes greater pressure drag and generates a boundary separation. There is then turbulence at the two ends of the deflector; in the left chamber and the upper right chamber.

The ongoing hot air changes direction after encountering the deflector, and forms turbulence in the left chamber through interaction with the wall. Hot air enters the right chamber of the drying oven through the channel. A large quantity of hot air then moves forward from the back of the drying oven and a little of the hot air goes to the right. This generates a collision of hot air from two different directions and a collision of hot air with the wall. Furthermore, the inlet is close to the upper right of the chamber, which is a comparatively small space. Turbulence is therefore generated here in the right chamber. In addition, the trace map shows clearly that there is more hot air flow in the inlet pipe, due to the influence of different air intake methods in the left and right chambers [16].

### 3.2 Hot-air pressure analysis in a drying oven

Figure 6 shows a pressure vector diagram of a drying oven where hot air is divided into two passages, which are then blown to air dividing channels at both sides, after entering tuyeres via an air suction port [17]. After being divided via the tuyeres, the hot air is blown to the substrate surfaces from the five rows of tuyeres.

As shown, the uniformity of hot air blowing is mainly determined by the structure of the oven, such as the width of the air channels at both sides and the area of the connection part [18]. The following conclusions can be made:

Firstly, the pressure difference between the tuyeres at the two ends is rather large. Pressure close to the suction port is large and the hot-air speed is correspondingly high, while pressure at the other end is small and the corresponding air blowing velocity is low.

Secondly, hot-air speed is mainly determined by the pressure of the oven, the change of which is shown in Figure 6. Hot-air speed tends to decrease along the air blowing direction of tuyeres. To ensure equal air blowing velocity through tuyeres, proper measures should be taken to reduce pressure differences between two rows of tuyeres, so that the pressure of all the incoming ducts tends to uniformity. This is to ensure consistency of pressure from the middle of air tubes and finally to achieve the objective of a uniform velocity in the five rows of tuyeres.

As stated above, hot air is sent into tuyeres inside the drying device, via the air suction port. It is then sent into two rows of tuyeres by flow guide plates. Whether the distribution of air pressure at the two sides is rational will directly affect the uniformity of air blowing in the tuyeres and will finally affect the air blowing velocity of various rows of tuyeres.

## 4. STRUCTURE OPTIMIZATION OF A DRYING OVEN

### 4.1 Structure optimization of air ducts

According to analysis of the results in Section 4, the pressure difference between the incoming air ducts of the drying device and the structure is large. This severely affects the uniformity of air speed. The following solutions are therefore raised to modify the structure of the air ducts.

The bottoms of both rows of air ducts are connected together, so that hot air flows can be connected with each other at the bottom, as shown in Figure 7. The connection height is  $H=200$  mm. Modification of the air ducts whose upper and lower portions are connected together overcomes the defect of a single connected air duct in the existing structure, which effectively improves non-uniform air blowing [19][20].

The pressure distribution is shown in Figure 8. A connecting air duct with a uniform pressure is provided for both the upper and lower air ducts. In the two groups of air ducts, the upper connected air ducts are primary air ducts and the lower air ducts mainly play the role of unifying air pressure at the bottom of the air ducts.

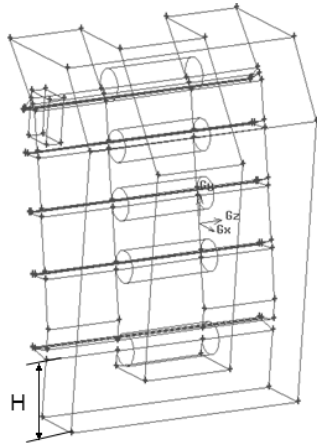


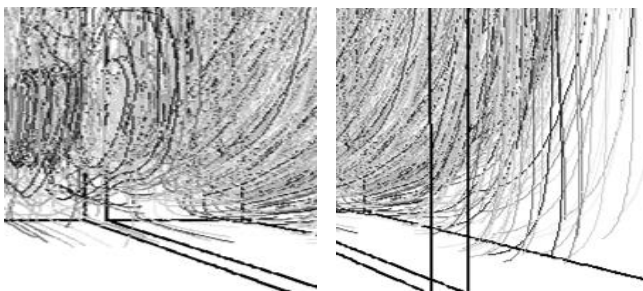
**Figure 7.** Structure of the optimization of air ducts



**Figure 8.** Pressure distribution of the optimization structure

#### 4.2 Position optimization of the air blowing port

The position of the air blowing port is very important. If its position is selected irrationally, hot air finishing drying cannot be exhausted on time. This can very easily cause solvent retention and can also lead to the content of organic solvent in the drying device exceeding minimum values [21].



(a) Original (b) Optimization

**Figure 9.** Trace map of a drying oven bottom

As shown in Figure 9(a), hot air forms a whirlpool at the bottom of the drying device, so that hot air is difficult to exhaust; causing the problem of organic solvent retention. Organic solvents in ink are easy to volatilize and belong to a group of inflammable and explosive substances. The concentration of organic solvents in the drying device should therefore be controlled strictly [22].

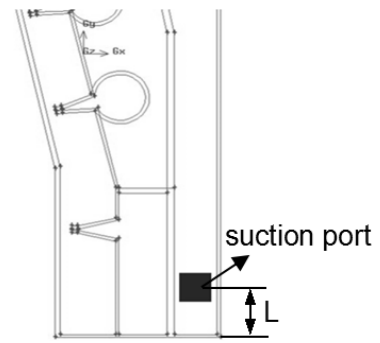


**Figure 10.** Location of the air suction port

It is found, through simulation analysis of the whole system, that the distance ( $L$ ) from the center of the whirl to the bottom of the drying device is 26cm. That is to say, organic solvents can easily accumulate there, which will affect the substrate quality. Therefore, an air suction port is added at the point  $L=26\text{cm}$ . This is far enough away from the bottom of the drying device to eliminate the defect, to ensure quality of substrates, and to effectively decrease the explosion risk from organic solvents. The structure of the air suction port is shown in Figure 10.

A trace map of the hot air flow is shown in Figure 9(b). It is easy to see that the flow state of the hot air at the bottom is approximate to laminar flow, which effectively solves the problem of organic solvent retention.

## 5. STRUCTURE OPTIMIZATION OF TUYERES

### 5.1 Flat clapboard structure optimization

To improve the non-uniform circulation of hot air between the tuyere and to increase utilization efficiency, this paper puts forward a new structure for tuyeres, with a horizontal clapboard, as shown in Figure 11.

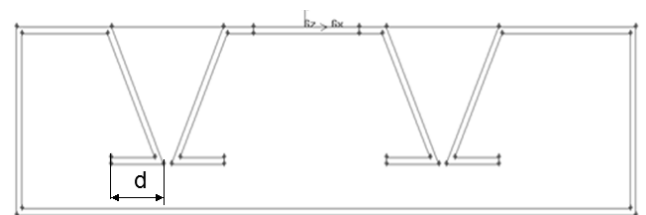


**Figure 11.** Flat clapboard structure

The lengths of the horizontal clapboards are: 6 mm, 8mm, 12mm, 18mm, 24mm and 30mm. The structural dimensions and average air speed in the substrate are shown in Table 1.

**Table.1** Clapboard length corresponding to air speed

d (mm)	6	12	18	24	30
s (m/s)	6.97	7.53	8.14	9.67	13.71

As shown in Figure 12(a), when the length of the horizontal clapboard ( $d$ ) was 12mm, after being blown via tuyeres, most hot air could not stay on the surfaces of the substrate for long,

and flowed directly to the air outlet. In Figure 12(b), the clapboard length is increased to 24mm. The flow track of hot air gradually forms a convolution on the surfaces of the substrate, which greatly increases the utilization efficiency of hot air [9]. Convolution is also beneficial for increasing the flow velocity of hot air on the substrate surfaces, so that the ink drying speed is noticeably increased and substrate drying is more uniform [23].

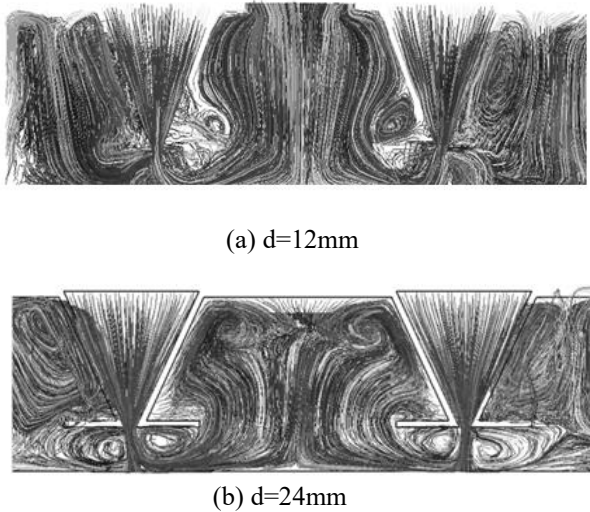


Figure 12. Hot-air trace maps for different clapboards

Figure 13 shows the pressure distribution of hot air. As shown, when the clapboard length is 24mm, air pressure of the tuyeres corresponding to the substrate is rather uniform. It can therefore be assumed that drying of the substrate by the structure will be more uniform.

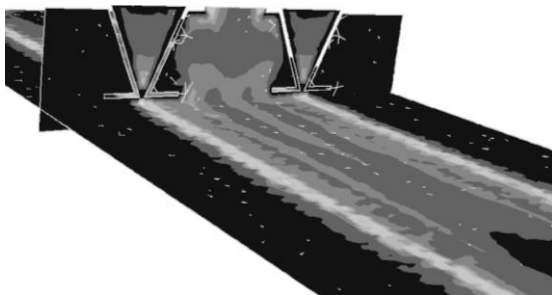


Figure 13. Hot-air pressure as d=24mm

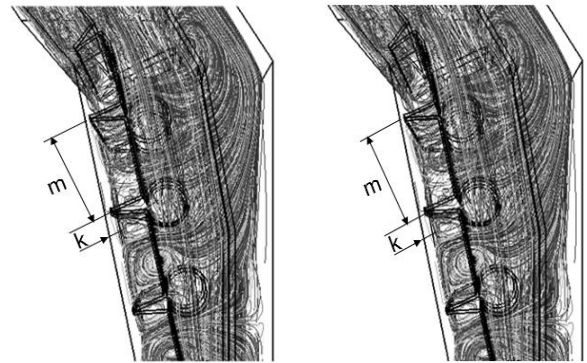
If only uniformity and the retention time of hot air on substrate surfaces are considered, the retention time of hot air is the longest and the pressure of hot air on substrate surfaces is relatively uniform when the horizontal clapboard length is 30mm. However, the inner pressure of the oven body under the structure also increases noticeably. This can very easily cause solvent retention and will also generate unfavorable effects on the exhaust of hot air. The structure with a 30mm length of horizontal clapboard should therefore be rejected [24] [25].

## 5.2. Interval of tuyeres

The interval of tuyeres has a very important influence on the uniformity and stability of hot air inside the drying device [26]. An irrational interval of tuyeres may cause a decreased

utilization efficiency of hot air and subsequent residual solvent. Intervals of tuyeres and paper space are shown in Figure 14.

Through comparative analysis and attempts with nine different structures, this paper finds that the vortex flow formed by the structure with  $m=160\text{mm}$  of internal and  $k=10\text{mm}$  of paper space on the substrate surfaces is significant. The hot air has a long retention time on the substrate and the air blowing speed is uniform.



(a)  $m=120\text{mm}$  (original) (b)  $m=160\text{mm}$  (optimization)

Figure 14. Hot-air trace maps of different intervals of tuyeres

## 6. CONCLUSION

This paper established a hot-air drying system model based on an analysis of drying methods and mechanisms. The analysis was carried out using hot-air flow characteristics in an oven, through CFD simulation. The structure optimization is put forward as follows:

- (1) A connecting air duct with  $H=200\text{mm}$  could provide uniform pressure for hot air;
- (2) The structural addition of an air suction port at  $L=26\text{mm}$  could be beneficial in effectively controlling organic solvent retention;
- (3) A new tuyere, with a horizontal clapboard of  $d=24\text{mm}$ , could form convolutions which would improve drying speed, the utilization of hot-air efficiency, and drying uniformity.

- (4) A structure with internal  $m=160\text{mm}$  and  $k=10\text{mm}$  of paper space to the substrate surfaces is significant for increasing drying efficiency of the substrate and for efficiently decreasing solvent residue.

This research therefore provides certain instructions for optimization in the design of drying ovens in the future.

## ACKNOWLEDGMENTS

The author gratefully acknowledges the support of the National Natural Science Foundation of China (Grant No.51375395), China Postdoctoral Science Foundation (2014M552484), Natural Science Foundation of Shaanxi Province (2014JM8334), Science Foundation of Shaanxi Educational Department (Natural Science 2013jk0996), and Science Foundation of Xi'an University of Technology (104-211106).

## REFERENCES

1. Jiangyan Bei, *Gravure Printing*, Chemical Industry Press, 2008.
2. Zonglei Xu, *Analysis of Fluid Dynamic Characteristic Analysis and Parameter Optimization of Drying Device in a Gravure Printing Machine*, Xi'an University of Technology, 2011.
3. Jian Liu, *Analysis and Structure Optimization of Hot Air Drying Device in a Gravure Printing Machine*, Xi'an University of Technology, 2011.
4. Weili Wang, Wenge Chen, "The analysis on drying system of gravure press", *Journal of Packaging Engineering*, Vol.6:98-100, 2008.
5. Peiyong Feng, *Parameter Optimization of Dry System of Plastic Gravure Printing Machine*, Xi'an University of Technology, 2006.
6. Ani Wang, *Parameter Optimization of Plastic Gravure Printing Machine Hot Air Drying*, Xi'an University of Technology, 2008.
7. Xianwen Shen, *The Hot-air Fluid Dynamic Analysis and Structure optimization of the YF93 Oven for the Gravure printing machines*, Xi'an University of Technology, 2013.
8. Jing Wang, *Basis of Heat Transfer and Fluid Dynamics*, Shanghai Jiaotong University Press, 2007.
9. Linlin Liu, Jian Liu, Xiaoyan Zhang, Shanshan Zheng, "Analysis and optimization of hot air drying device of a gravure printing machine based on fluid analysis," *Applied Mechanics and Materials*, Vol.121:2517-2521, 2012.
10. Linlin Liu, Rong Mo, Neng Wan, "Machining process & information modeling based on mbd procedure machining cell," *Manufacturing Technology*, Vol.15, No.2,2015
11. Autel, *Basis of Prandtl Fluid Dynamics*, Science Press, 2008.
12. Best Practice Guidelines, *Version 1.0, ERCOFTAC Special Interest Group on "Quality and Trust in Industrial CFD"*, January, 2000.
13. Linlin Liu, Zhengcheng Sun, Chuliang Wan, Jimei Wu, "Jet flow field calculation & mechanism analysis on hot-air drying oven based on RNG K-E model," *International Journal of Heat and Technology*, Vol.33:77-82, 2015.
14. Bruno Eck.Fans, *Design and Operation of Centrifugal, Axial-Flow and cross-Flow Fans*, Pergamon Press LTD, 1973.
15. S.Kakac, A.E.Bergles, F.Mayingner, *Heat Exchangers-Thermal-Hydraulic Fundamentals and Design*, McGraw-Hill, 1980.
16. Anderson J.D, *Computational Fluid Dynamics: the basics with applications*, McGraw-Hill, 1995.
17. J.P. Van Doormal, G.G. Raithby, "Enhancement of the SIMPLE method for predicting incompressible fluid flows," *Numerical Heat Transfer*, Vol.7:147-163, 1984. DOI: [10.1080/10407798408546946](https://doi.org/10.1080/10407798408546946).
18. Versteeg H.K., Malalasekera W., *An Introduction to Computational Fluid Dynamics: the finite volume method*, England: Longman Group Ltd, 1995.
19. C. F. Ma, Q. Zheng, H. Sun, K. Wu and K.Horii, "Local convective heat transfer from a vertical flat surface to oblique submerged impinging jets of large Prandtl number liquid," *Experimental Thermal and Fluid Science*, Vol.17(23): 8-247, 1998.
20. PICH AVANT L., "Optimization of a UV curable acrylate-based protective coating by experimental design," *Progress in Organic Coatings*, Vol.63 (1): 55-62, 2008.
21. Linlin Liu, Rong Mo, Neng Wan, Yibo Huang, "Process knowledge of procedure machining cell modeling: On the basis of factor space theory," *International Journal of Earth Sciences and Engineering*, Vol.7,2015
22. Lindfield G., Penny J., *Numerical Methods Using MATLAB, 2nd ed*, NJ: Prentice Hall, 2000.
23. Yinhe Jin, *Flexography printing*, Chemical Industry Press, 2001.
24. Hui Song, Ying Pan, "Application of far infrared radiation and hot air convection drying," *China Bicycle*, 3:23-25, 1996.
25. Linlin Liu, Rong Mo, Neng Wan, "A MBD procedure model based on machining process knowledge," *International Journal of Applied Mathematics and Statistics*, Vol.51, 2013.
26. Qingming Huang, Fangyuan Chen, Nengheng Bao, Peng Xu, Wenhua Bai, "Research and design for temperature optimized control system of drying oven to gravure press," *Journal of Manufacturing Informatization*, 8:23-45, 2008.